GFDM Frame Design For 5G Application Scenarios

Juliano Ferreira, Henry Rodrigues, Arturo González, Ahmad Nimr, Maximilian Matthe, Dan Zhang, Luciano Mendes and Gerhard Fettweis

***Abstract*—The services foreseen for 5G networks will demand a vast number of challenging requirements to be fulfilled by the physical layer. These services can be grouped into application scenarios, each one with a key requirement to be addressed by the 5G network. A flexible waveform associated with a appropriate data frame is an essential feature in order to guarantee the support of contrasting requirements from different application scenarios such as Enhanced Mobile Broadband, Internet of Things, Tactile Internet and Internet Access for Remote Areas. In this paper, we propose a flexible data frame based on Generalized Frequency Division Multiplexing (GFDM) that can be tailored to address the specific key requirements of the different 5G scenarios. The paper also presents the physical layer parametrization that can be used for each application.**

***Index Terms*—5G networks, data frame, frame design, application scenarios, GFDM.**

I. INTRODUCTION

CELLULAR terminals have evolved from devices providing voice connectivity to source and sink for multimedia, sensor, positioning and other varied digital content. Nowadays, several new application scenario are being considered for fifth generation of mobile network (5G) and each one has a key requirement to be addressed. Enhanced Mobile Broadband (eMBB) is the natural evolution of fourth generation of mobile network (4G), where the aim is to provide data rates up to 10 Gbps [1]. Ultra Reliable Low Latency (URLL) applications, also known as Tactile Internet [2], requires latency below 1 ms and robustness in order to avoid packages retransmissions. The Internet of Things (IoT) and Machine-Type Communication (MTC) will demand connectivity of a massive number of energy-limited devices per cell [3], which cannot afford cumbersome synchronization process with the network. Internet Access for Remote Areas (IARA) is the last frontier for universal connectivity and 5G must present a operation mode capable of supplying Internet connect in remote/rural areas, where the cell coverage must be bigger than 50 km [4] and, therefore, over a doubly-dispersive channel [5].

It is clear that these contrasting requirements do not need to be simultaneously fulfilled. 5G networks are expected to have different operation modes, each one designed for one specific application scenario. The base station (BS) computational resources, as well the time and frequency grid need to be dynamically allocated for the different application scenarios, depending on the users' demands. A new concept, defined as network slicing [6], allows for sharing the communication and processing resources of a 5G BS among the different 5G services. Each operation mode could have a specific physical layer (PHY). However a unified data frame, based on a flexible waveform able to address the different 5G requirements would simplify the network management and deployment of future services. Therefore, the approach based on a single waveform is preferred over the approach based on a multitude of specific PHYs.

Several new waveforms have been recently proposed for 5G networks [7]. Filterbank Multicarrier (FBMC) [8] relies on linear filtering per subcarrier and Offset Quadrature Amplitude Modulation (OQAM) to mitigate the intercarrier interference (ICI), achieving high spectrum efficiency and very low out-of-band emission (OOBE). However, the long filter tails hinder the usage of this waveforms in situations where a short burst of data needs to be transmitted, such as MTC and IoT applications. Universal Filtered Multi-Carrier (UFMC) [9], also known as Universal Filtered Orthogonal Frequency Multiplexing (UF-OFDM), is an Orthogonal Frequency Division Multiplexing (OFDM) [10] based waveform, where a short length filter is used to filter a set of subcarriers, which remain orthogonal to each other within the filter's subband. UFMC does not use cyclic prefix (CP) to combat intersymbol interference (ISI) and zero-padding is employed to accommodate the filter spreading. Therefore, UFMC is more sensitive to time misalignments, resulting in performance loss even when small time synchronization errors occur [9]. Filtered Orthogonal Frequency Division Multiplexing (F-OFDM) [11] is another OFDM-based waveform that also employs subband filtering. But, unlike UFMC, F-OFDM uses CP to avoid ISI in multipath channels. F-OFDM can achieve low OOBE and the CP allow for small time synchronization errors without performance penalty. However, like OFDM, F-OFDM employs one CP per symbol, reducing the spectrum efficiency specially when short symbols are required, i.e., in URLL applications. Generalized Frequency Division Multiplexing (GFDM) [12] is another 5G candidate waveform that, like FBMC, employs subcarrier-based filtering to reduce OOBE. However, GFDM uses circular filtering in time and frequency domains, meaning that the filter spreading is confined with the GFDM symbol. In this case, K subcarrier, each one composed by M subsymbols, are used to transmit $N = KM$ quadrature amplitude modulation (QAM) data symbols. CP and cyclic suffix (CS) can be used to protect the symbols against the multipath channels.

Among these candidates, GFDM has been shown to represent a trade-off between complexity and performance, as-

J. Ferreira, H. Rodrigues and L. Mendes are with Instituto Nacional de Telecomunicações, Santa Rita do Sapucaí, MG, Brazil.
(e-mail:{silveira, henry, luciano}@inatel.br)
A. González, A. Nimr, M. Matthe, D. Zhang and G. Fettweis are with Vodafone Chair Mobile Communication Systems, Technische Universität Dresden, Germany. (e-mail:{arturo.gonzalez, ahmad.nimr, maximilian.matthe, dan.zhang, fettweis}@ifn.et.tu-dresden.de)
The Associate Editor coordinating the review of this manuscript and approving it for publication was Prof. Renato Machado.
Digital Object Identifier: 10.14209/jcis.2017.6

suming the different requirements imposed on 5G networks [13]. GFDM symbol can be shrunken to reduce latency, while keep the efficient usage of the CP, and it can be precoded with Walsh-Hadamard Transform (WHT) to increase robustness for URLL application [14]. Time-windowing and blank subsymbols [15] can be used to reduce even further the OOBE, trigging dynamic and fragmented spectrum allocation [16] required for IARA and eMBB applications. The usage of CP and CS protects the GFDM symbol of small timing synchronization errors. Because of the high flexibility and the acceptable performance for all foreseen application scenario, we have selected GFDM as the waveform to be employed in the 5G frame design.

The aim of this paper is to present a flexible PHY frame, based on the GFDM features, that can be used to properly address the requirements of the different 5G scenarios. The proposed PHY frame can be adjusted to achieve high spectrum efficiency, low latency, synchronization robustness and high protection against multipath channels. The paper also brings a set of PHY parameters that can be employed to support each application scenario, showing that an unified PHY frame based on GFDM can be used to fulfill the 5G demands.

This paper is organized as follows: section II brings the application scenarios and the corresponding requirements, while section III presents the GFDM principles. Section IV describes the frame design methodology and section VI proposes the parametrization of the PHY for each application scenario. Finally, section VII concludes the paper.

II. Scenarios for 5G

The main characteristic of 5G network is that it must support services that differ greatly in their communication requirements and performance targets. These services can be organized in application scenarios sharing similar requirements in terms of throughput, latency and reliability [1] [17]. The main 5G application scenarios are briefly described next.

A. Enhanced Mobile Broadband (eMBB)

This scenario can be seen as an evolution of the current 4G networks, since its main objective is providing higher throughput of up to 10 Gbps. End-to-end latency should not exceed 10 ms for multimedia traffic. Cell radius of up to one kilometer can be assumed in urban areas. The main techniques that are being considered to support these requirements are millimeter wave combined with massive multiple-input multiple-output (MIMO) [18] [19], cooperative multi-point (CoMP) [20] and high spectrum efficient waveform with low OOBE [12].

B. Ultra Reliable Low Latency (URLL)

The mission-critical URLL aims for high reliable low latency services, where the low end-to-end latency must be less than 1 ms. This requirement means that the overall frame size must be limited, implying in a restricted forward error control (FEC) length [21]. This is a very challenging situation, since a robust FEC must guarantee low bit error rate (BER) and Automatic repeat request (ARQ) [22] cannot be used due to the latency requirement.

C. Internet of Things (IoT) / Machine-Type Communication (MTC)

IoT/MTC will play a key role in the definition of 5G networks. This scenario is being pointed as the main opportunity for new revenues for telecommunication operator. The number of devices connected to the network (over 50,000 devices per cell) [1] and long battery life time (above 10 years) are the key requirements of this scenario. Low energy consumption, loose synchronization procedure and random channel access are some features that the PHY must provide for this application scenario. The peak data rate considered is between 1 kbps to 10 Mbps. Latency requirements vary from 1 to 100 ms in order to cover a broad range of applications, from the demanding industrial automation to smart metering.

D. Internet Access for Remote Areas (IARA)

IARA basically demands large cellular coverage in order to increase the number of subscribers per cell in rural and low populated areas. Opportunistic dynamic and fragmented spectrum allocation is a key feature in this scenario. The PHY must be based on a waveform that can efficiently exploit the CP in order to achieve high spectrum efficiency under channels with long delay profile. Also, the peak data rate and end-to-end latency that it can provide should be comparable to Long-Term Evolution (LTE), i.e. 100 Mbps and latency of 50-100 ms.

Table I summarizes the requirements of foreseen 5G application scenarios.

TABLE I
5G requirements.

Requirement	eMBB	IoT	URLL	IARA
Data Rate (Mbps)	$\leq 10^4$	$10^{-3} \sim 10$	≤ 1	≤ 10
Latency (ms)	≤ 10	$1 \sim 100$	≤ 1	$50 \sim 100$
Cell (Km)	$0.1 \sim 1$	≈ 10	$0.1 \sim 1$	≈ 50
Speed (km/h)	≤ 8	$0 \sim 50$	4	$0 \sim 50$
FEC	yes	yes	yes	yes
ARQ	yes	no	no	yes

III. GFDM Model

Assume that a GFDM block occupies K subcarriers, each one carrying M data symbols, which are temporally equally spaced and circularly filtered by a prototype filter $g[n]$ with $N = KM$ samples. The GFDM block is given by

$$x[n] = \sum_{k \in \mathcal{K}_{\text{on}}} \sum_{m \in \mathcal{M}_{\text{on}}} d_{k,m} g\left[\langle n - mK \rangle_N\right] e^{j2\pi \frac{k}{K} n}, \qquad (1)$$

where $d_{k,m}$ is a QAM symbol, $\langle a \rangle_b$ stands for the a modulo b operator and $\mathcal{K}_{\text{on}}$ and $\mathcal{M}_{\text{on}}$ are the sets of active subcarrier and subsymbols, respectively. As illustrated in Fig. 1, it is possible to arbitrarily insert the QAM symbols in the GFDM time-frequency grid. Hence, a GFDM symbol carries $N_{\text{on}} = M_{\text{on}} K_{\text{on}}$ data symbols, where M_{on} and K_{on} are the cardinalities of $\mathcal{K}_{\text{on}}$ and $\mathcal{M}_{\text{on}}$, respectively.

Analogous to OFDM, GFDM also adopts CP to mitigate multipath channels, but a single CP is used to protect M_{on}

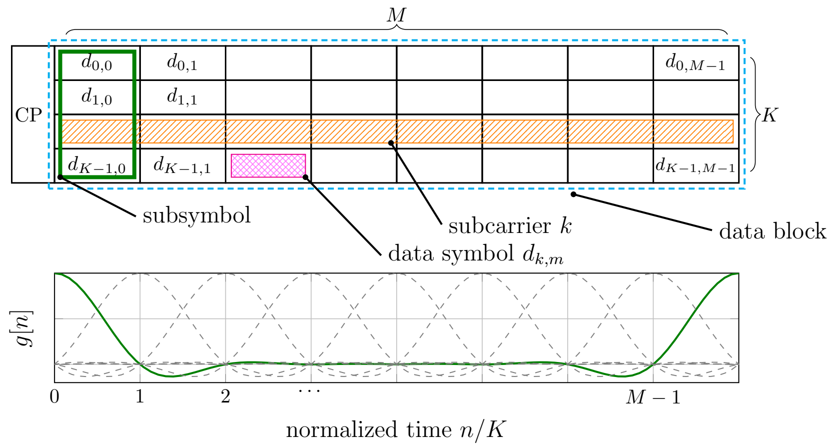

Fig. 1. Time-frequency grid of GFDM and terminology.

subsymbols, significantly increasing the spectrum efficiency when M_{on} is large, e.g. $M_{\text{on}} \geq 5$.

Another interesting GFDM feature is that this waveform can cover the 4G waveforms, i.e., OFDM and DFT spread OFDM (DFT-s-OFDM), as corner cases. OFDM is obtained by making $M = 1$ and using a square pulse as prototype filter, while DFT-s-OFDM is obtained when $K = 1$ and using a Dirichlet pulse as prototype filter. Therefore, GFDM can also be employed in hybrid 4G-5G system during the standard transition, smoothing the transition to a new standard, while still offering support for legacy users.

GFDM offers additional degrees of freedom for enhancing the waveform performance. Peak to average power ratio (PAPR) of DFT-s-OFDM can be reduced by increasing the roll-off factor [23] and the OOBE can be reduced by leaving blank subsymbols in the head and tail of the GFDM block [12]. Time-domain windowing can further reduce the OOBE [15]. Using circular rather than linear filtering, GFDM produces symbols that are well localized in time, which makes GFDM robust against time misalignment. Hence, the flexibility offered by GFDM makes it an attractive solution to achieve a unified air interface for diverse 5G scenarios.

IV. GFDM-based Frame: Proposed Data Structure

The PHY structure for the 5G PHY must allow a flexible resource allocation into the M_{on} subsymbols of the the K_{on} subcarriers, considering all required overhead, such as coding rate, synchronization preambles, CP and CS. Figure 2 depicts the frame structure proposed in this paper and the terminology used to identify each element of the frame.

The code word length is an important parameter with a trade-off between correction performance and latency. The final code word is mapped into

Consider a bit sequence with length k_{L} representing the uncoded PHY payload, which consists of user data and upper layer headers. A channel coding of rate $R_{\text{C}} = k_{\text{L}}/n_{\text{L}}$ is employed to form a code-word with length of n_{L} bits. The bits of the code-word are mapped into a M_{C}-QAM constellation, where M_{C} is the modulation order. This QAM sequence is defined as FEC Block. Fig. 2.a describes this data flow. It is assumed that n_{L} is fixed for a given scenario.

Let's $N_{\text{QAM}} = n_{\text{L}}/\log_2(M_{\text{C}})$ be the number of QAM symbols within a FEC Block. Clearly, N_{QAM} is not necessarily equal to the number of the active data symbols N_{on} within one GFDM symbol. Therefore, N_{FEC} FEC blocks, containing $N_{\text{FEC}}N_{\text{QAM}}$ QAM symbols, are mapped into N_{G} GFDM symbols (or GFDM resource blocks), which has the capacity to carry $N_{\text{G}}N_{\text{on}}$ QAM symbols, as shown in Fig. 2.b. Therefore,

$$N_{\text{G}}N_{\text{on}} = N_{\text{FEC}}N_{\text{QAM}} \tag{2}$$

must hold.

The frame is generated based on the smallest N_{FEC} that satisfies (2). This can be evaluated as

$$N_{\text{FEC}} = \frac{\text{LCM}(N_{\text{on}}, N_{\text{QAM}})}{N_{\text{QAM}}}, \tag{3}$$

where $\text{LCM}(a, b)$ returns the *Least Common Multiple* of a and b.

Now, considering that preamble-based synchronization and channel estimation are employed, a frame is generated by time-multiplexing N_{G} modulated GFDM symbols (N_{FEC} FEC blocks) with N_{P} preambles. The waveform employed as preamble is known by the receiver and it has the same spectral and time properties of the GFDM signal. The preamble spectral content spreads through the desired bandwidth and the time interval between two successive preambles must be smaller than the channel coherence time. Clearly, increasing the number of preambles per frame eases the synchronization process and improve channel tracking, but at the cost of throughput reduction. The frame duration is given by

$$T_{\text{F}} = N_{\text{G}}T_{\text{G}} + N_{\text{P}}T_{\text{P}}, \tag{4}$$

where T_{P} is the preamble duration and T_{G} is the GFDM symbol duration, which is expressed as

$$T_{\text{G}} = \frac{S_{\text{GS}}}{F_{\text{S}}} = \frac{S_{\text{RB}} + S_{\text{CP}_\text{e}} + S_{\text{CP}_\text{W}} + S_{\text{CS}_\text{W}}}{F_{\text{S}}}, \tag{5}$$

with S_{GS} being the number of samples per GFDM symbol and F_{S} being the sampling frequency. S_{RB} is the number of

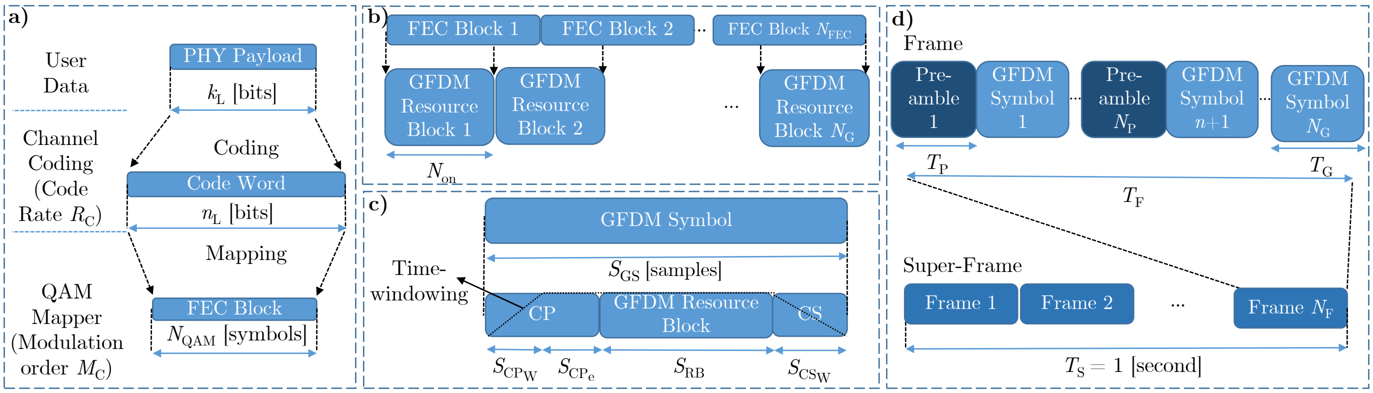

Fig. 2. GFDM-based Frame Design a) FEC Block composition. b) FEC Block encapsulation on GFDM Resource Blocks; c) GFDM Symbol sample length; d) Frame and Super-Frame composition and time duration.

samples per GFDM resource block, S_{CP_e} is the number of CP samples effectively used to combat the multipath channel, S_{CP_W} and $_{CS_W}$ are the number of samples of the CP and CS, respectively, that are used for time-windowing. Fig. 2.c illustrates the composition of a GFDM symbol. Similarly T_P can be calculated from its corresponding CP and CS parameters.

MIMO is an essential technique for 5G systems. Time-Reverse Space Time Coding (TR-STC) [24] can be applied on groups of GFDM symbols, in order to achieve transmit diversity. The data frame proposed in this paper allows for adjusting the number of preambles that are transmitted by each antenna. On the proposed scheme, all transmit antennas sends preambles simultaneously, assuming that the receivers have two or more receive antennas. TR-STC is not applied on the preambles and the channel state information can be estimated on all receiving antennas using minimum mean square error (MMSE) or zero-forcing (ZF) [12], depending on the complexity that the receiver can afford.

Finally, an integer number of frames are concatenated, resulting in a super-frame as depicted in Fig. 2.d, which has the exact duration of 1 second. Assuming the base station have access to the global positioning system (GPS) system, the super-frame may be locked to the 1 pulse per second (1PPS) signal. When the receiving device also has access to the GPS signal, time and frequency synchronization is easily acquired with a 1PPS-aided scheme. Likewise, when the receiver is synchronized with the base station, a fast GPS location is acquired with a GFDM-aided scheme. Usually, tens of seconds are spent to discipline a local oscillator based on the received 1PPS signal, in order to acquire an accurate location. The energy and time spent on synchronization can be safe if a local oscillator derived from the GFDM symbol is already locked to the GPS system.

In order to guarantee the super-frame fits exactly in 1 second, GFDM symbol and preamble duration time must be accurately adjusted by the varying number of samples in CS and/or CP. Therefore, the integer number of frames in a super-frame is given by

$$N_F = T_S/T_F, \tag{6}$$

where T_S is the super-frame duration, which is fixed to 1 second for convenience.

V. Performance Criteria for 5G

The parametrization of the GFDM frame for each 5G application scenario depends on the key requirement that needs to be addressed. Following we describe the relationship between the requirements and the system parameters.

1) System bandwidth: The bandwidth of the resultant GFDM signal is given by

$$B_W = \frac{F_S K_{on}}{K}. \tag{7}$$

2) PHY Gross bit rate: The total bit rate transmitted by GFDM symbols is given by

$$R_B = \frac{R_C N_F N_G N_{on} \log_2(M_C)}{T_S}. \tag{8}$$

3) Spectral efficiency: The spectral efficiency of the system is given by $\varepsilon = R_U/B_W$. Based on Shannon's theorem for channel capacity and assuming a coding scheme that leads to the optimum performance, the minimum signal-to-noise ratio (SNR) required for a given spectral efficiency under additive white Gaussian noise (AWGN) channel [25] is

$$\mathrm{SNR_{min}} = 10\log_{10}\left(2^{\varepsilon} - 1\right). \tag{9}$$

4) PHY Latency: The system latency can be estimated based on the time transmission interval (TTI), which is the time interval required to the PHY to transmit one code-word. The average TTI can is approximately give by

$$T_{TTI} \approx T_F/N_{FEC}. \tag{10}$$

The one-way transit time of a FEC block can be roughly approximated by $3.5T_{TTI}$ [26]. Therefore, the round trip time (RTT) [27] is $T_{RTT} \approx 7T_{TTI}$.

5) Mobile speed: Considering channel state information is estimated on every preamble, the maximum supported mobile speed is determined by the time interval between preambles, which is given by

$$\Delta T_P = \frac{T_F}{N_P}. \tag{11}$$

The minimum channel coherence time is $T_C = \Delta T_P/0.7$, assuming a 70% confidence factor. The maximum Doppler frequency is $f_{D_{max}} \approx 0.423/T_C$ [28] and the maximum supported speed is $V_m = f_{D_{max}}\lambda_c$, where λ_c is the carrier wavelength [28].

6) Battery lifetime: In order to establish an approximate estimative of the impact from the frame design into the power consumption, a simplified consumption model based on [29] and [30] was applied on a mobile autonomous reporting (MAR) IoT device [31]. We assume periodic reports transmission without ARQ. In the adopted model, a MAR device stays on sleep mode most of the time and bursts data following the steps described next:
i) Warm-up to wake up from sleep; ii) Time and frequency synchronization; iii) Transmission of one FEC block (TTI); iv) Turning off the RF circuitry; and v) sleep considering 1 transmission per hour.
The power consumption analysis mentioned in this paper considers a 3.3 V battery with capacity of 6,500 Joules [30].

VI. GFDM-BASED FRAME: MEETING THE REQUIREMENTS OF EACH SCENARIO

Different 5G operation modes are necessary in order to address the key requirements of the application scenarios. In Table II, we propose four different parametrization of the GFDM frame presented in this paper. Each set of parameters aims for attending a specific 5G scenario.

TABLE II
GFDM-FRAME PARAMETRIZATION FOR THE 5G SCENARIOS.

Parameter	Scenario				Unit
	eMBB	URLL	IoT	IARA	
F_S	30.72	30.72	0.96	30.72	MHz
n_L	64800	480	480	64800	bits
R_C	0.833	0.533	0.533	0.250	code rate
M_C	256	16	16	16	modulation order
GFDM symbol configuration					
K	128	32	4	2048	carriers
K_{on}	75	18	1	1200	carriers
K_{on} (Max. users)	38	9	1	600	carriers
$M = M_{on}$	15	7	15	15	subsymbols
S_{RB}	1920	224	60	30720	samples
S_{CP_e}	128	128	5	2048	samples
$S_{CP_W} = S_{CS_W}$	83	14	4	432	samples
GFDM-based preamble configuration					
K	128	128	16	1024	carriers
K_{on}	75	75	4	600	carriers
$M = M_{on}$	2	2	2	2	subsymbols
S_{RB}	256	256	32	2048	samples
S_{CP_e}	128	128	5	2048	samples
$S_{CP_W} = S_{CS_W}$	104	8	2	493	samples

The preamble used in this propose consists on a GFDM symbol with $M = M_{on} = 2$. The preamble load is formed by a sequence of K_{on} QAM symbols, which are repeated in each subsymbol. Tis preamble content creates a time-redundancy that can be exploited by the synchronization algorithm on the receiver side [32].

Tables III and IV summarize the frame parameters for each scenario and the achieved performance, respectively. The parameter R_k in Table IV represents the multipath robustness of the GFDM symbol, obtained as

$$R_k = \frac{S_{CP_e}}{F_S} c, \tag{12}$$

where c is the speed of light in vacuum. A 10 GHz carrier frequency has been considered to estimate V_m. R_k were defined considering that the multipath robustness is equivalent to 15 to 18% of the cell radius [33]. The preambles length were defined using this reasoning.

TABLE III
GFDM FRAME SPECIFICATION FOR EACH SCENARIO.

Param.	Scenario				Unit
	eMBB	URLL	IoT	IARA	
N_{QAM}	8100	120	120	16200	QAM symbols
N_{on}	1125	126	15	18000	QAM symbols
N_{on} (Max. users)	570	63	15	9,000	QAM symbols
$S_{GS\,G}$	2214	380	73	33632	samples
$S_{GS\,P}$	592	400	41	5082	samples
T_G	72.07	12.37	76.04	1094.79	μs
T_P	19.27	13.02	42.71	165.43	μs
T_F	10417	2500	1302	12500	μs
N_G	144	200	16	9	GFDM symbols
N_{FEC}	20	42	2	10	FEC blocks
N_P	2	2	2	16	preambles
N_F	96	400	768	80	frames

TABLE IV
SYSTEM PERFORMANCE FOR EACH SCENARIO.

Parameter	Scenario				Unit
	eMBB	URLL	IoT	IARA	
B_W	18	17.28	0.24	18	MHz
R_B	124.42	40.32	0.74	51.84	Mbps
R_u	103.68	21.50	0.39	12.96	Mbps
ε	5.76	1.24	1.64	0.72	bps/Hz
SNR_{min}	17.26	1.36	3.25	-1.89	dB
R_k	1.25	1.25	1.56	20.00	km
T_{RTT}	3.65	0.42	4.56	8.75	ms
V_m	6.16	25.85	52.57	51.93	km/h

Table V shows the performance parameters considering the maximum number of users or devices allocated simultaneously for the set of parameters given by Table II. It was considerate one carrier as guard between each user, resulting on the total number of carriers per GFDM Symbol K_{on} (Max. users) in Table II, and the total number of active data symbols transported by each GFDM Symbol N_{on} (Max. users) in Table III. In Table Table V, U_s represents the maximum number of users allocated per frame and R_u represents the associated data rate per user. U_r give the maximum rate allocation of users per second. Finally, the parameter U_b gives the maximum rate allocation of users per second per Hertz, obtained by U_r/B_W.

Next subsections summarize the achieved results for each application scenario.

A. eMBB parameters and performance analysis

The number of subcarriers, number of subsymbols, and sampling frequency were selected to be compatible with LTE [34]. The considered channel coding is an LDPC (64800, 54000) with $R_C = 0.83$. The 256-QAM is used to increase spectral

TABLE V
SYSTEM PERFORMANCE FOR MAXIMUM NUMBER OF USERS.

Param.	Scenario				Unit
	eMBB	URLL	IoT	IARA	
U_s	5,472	1,800	16	5,400	users per Frame
R_u	18.95	11.95	24.58	2.4	kbps
U_r	525312	720000	12288	432000	users/s
U_b	0.029	0.040	0.051	0.024	users/s per Hz

efficiency at the expense of higher SNR_{min}. The number of preambles per frame is adjusted to comply with the mobile speed specification.

The suggested configuration provides the highest bit rate and spectral efficiency among the considered scenarios. In order to comply with the 10 Gbps specification from Table I, it is necessary to consider multiplexing MIMO and wider channel bandwidth. Considering an available bandwidth of 200 MHz and the spectral efficiency of 6 bps/Hz, it is necessary to employ an 9×9 MIMO in order to achieve the expected peak data rate for this scenario. Massive MIMO scheme with considerably higher arrays has already been demonstrated [35].

B. URLL parameters and performance analysis

The key requirement in this scenario is latency. The selected code-word length is small, with 480 bits, in order to decrease the overall latency. Considering the receiver must wait for the complete GFDM symbol before demodulation takes place, the symbol duration T_G has to be short. This is achieved by adopting a small number of subcarriers and subsymbols for a given sampling frequency. Furthermore, the number of active symbols N_{on} is optimized to carry one FEC frame composed of N_{QAM} QAM symbols, thus minimizing the TTI. The suggested configuration provides the lowest latency in terms of RTT with T_{RTT} = 0.42 ms, being the smallest among the selected scenarios. The resulting TTI is T_{TTI} = 0.06 ms, being 16.7 times smaller than the LTE TTI.

C. IoT/MTC parameters and performance analysis

Considering IoT and MTC devices must present low power consumption and low cost, the low sampling frequency of 0.96 MHz was adopted, being a sub-multiple of 30.72 MHz. This procedure reduces the bandwidth while maintaining backward compatibility with LTE master clock. Note that GFDM was parameterized with K_{on} = 1, leading to a single carrier system with low PAPR. The code-word length is 480 bits, complying with short messages typically sent by IoT devices.

The battery life-time estimated for a IoT device operating in the proposed system is 13.45 years, calculated in according with the power consumption model presented in Section V, surpassing the required 10 years life time.

Considering the minimum resource allocation for one device is 1 subcarrier per frame,up to 8 devices can share one frame. The maximum number of devices that cab be allocated per second is evaluated as $8N_F$, resulting in up to 12288 different devices per second, given by U_r. Therefore, this scenario presents the best U_b among the considered scenarios. It complies with a big number of devices per cell required on this scenario.

D. IARA parameters and performance analysis

The main specification of the IARA scenario is the extended coverage radius, for which a long CP is required to deal with multipath propagation. The OOBE is another critical requirement, since opportunistic spectrum allocation may be required to reduce the spectrum costs. Time windowing, combined with GFDM, is used here to achieve low OOBE. We assume that the maximum propagation distance between different paths without generating inter-symbol interference is 20 km. The obtained cell radius complies with the required wide coverage area.

VII. CONCLUSIONS

The design of the next generation of cellular networks needs to provide support for a new set of services, organized in application scenarios, that demand very different communication requirements. The proposed frame structure exploits the GFDM flexibility to get a single transmission framework adapted to different services. A set of frame configurations were proposed to comply with each scenario and its analysis shows that the key requirements of the next generation of cellular networks can be effectively achieved by a flexible frame structure and waveform.

ACKNOWLEDGEMENTS

The computations were performed on a computing cluster at the Center for Information Services and High Performance Computing (ZIH) at TU Dresden. The work presented in this paper was partially sponsored by the Federal Ministry of Education and Research within the programme "Twenty20 - Partnership for Innovation" under contract 03ZZ0505B - "fast wireless".

This work was supported by the German Science Foundation (DFG) within the priority program “Cooperative Interacting Cars (CoInCar)” (SPP 1835) and it was also supported by CNPq-Brasil and Finep/Funttel/Radiocommunication Reference Center under Grant No. 01.14.0231.00 hosted by Inatel.

REFERENCES

[1] A. Osseiran, F. Boccardi, V. Braun, K. Kusume, P. Marsch, M. Maternia, O. Queseth, M. Schellmann, H. Schotten, H. Taoka, H. Tullberg, M. A. Uusitalo, B. Timus, and M. Fallgren, “Scenarios for 5G mobile and wireless communications: The vision of the METIS project,” *IEEE Communications Magazine*, vol. 52, no. 5, pp. 26–35, 2014, doi:10.1109/MCOM.2014.6815890.

[2] G. Fettweis, “The Tactile Internet: Applications and Challenges,” *IEEE Vehicular Technology Magazine*, vol. 9, no. 1, pp. 64–70, March 2014, doi:10.1109/MVT.2013.2295069.

[3] M. Shirvanimoghaddam, M. Dohler, and S. J. Johnson, “Massive multiple access based on superposition raptor codes for cellular m2m communications,” *IEEE Transactions on Wireless Communications*, vol. 16, no. 1, pp. 307–319, Jan 2017, doi:10.1109/TWC.2016.2623305.

[4] A. Kumar, A. Karandikar, G. Naik, M. Khaturia, S. Saha, M. Arora, and J. Singh, “Toward enabling broadband for a billion plus population with tv white spaces,” *IEEE Communications Magazine*, vol. 54, no. 7, pp. 28–34, July 2016, doi:10.1109/MCOM.2016.7509375.

[5] K. Wang, X. Sha, and L. Mei, "On interference suppression in doubly-dispersive channels with hybrid single-multi carrier modulation and an mmse iterative equalizer," *IEEE Wireless Communications Letters*, vol. 1, no. 5, pp. 504–507, October 2012, doi:10.1109/WCL.2012.071612.120359.

[6] X. Zhou, R. Li, T. Chen, and H. Zhang, "Network slicing as a service: enabling enterprises' own software-defined cellular networks," *IEEE Communications Magazine*, vol. 54, no. 7, pp. 146–153, July 2016, doi:10.1109/MCOM.2016.7509393.

[7] G. Wunder, P. Jung, M. Kasparick, T. Wild, F. Schaich, Y. Chen, S. Brink, I. Gaspar, N. Michailow, A. Festag, L. Mendes, N. Cassiau, D. Ktenas, M. Dryjanski, S. Pietrzyk, B. Eged, P. Vago, and F. Wiedmann, "5GNOW: non-orthogonal, asynchronous waveforms for future mobile applications," *IEEE Communications Magazine*, vol. 52, no. 2, pp. 97–105, February 2014, doi:10.1109/MCOM.2014.6736749.

[8] B. Farhang-Boroujeny, "OFDM versus filter bank multicarrier," *IEEE Signal Processing Magazine*, vol. 28, no. 3, pp. 92–112, 5 2011, doi:10.1109/MSP.2011.940267.

[9] V. Vakilian, T. Wild, F. Schaich, S. Brink, and J.-F. Frigon, "Universal-filtered multi-carrier technique for wireless systems beyond LTE," in *Proc. Globecom 2013 9th International Workshop on Broadband Wireless Access*, Dec. 2013, doi:10.1109/GLOCOMW.2013.6824990.

[10] J. A. C. Bingham, "Multicarrier modulation for data transmission: an idea whose time has come," *IEEE Communications Magazine*, vol. 28, no. 5, pp. 5–14, May 1990, doi:10.1109/35.54342.

[11] P. Weitkemper, J. Bazzi, K. Kusume, A. Benjebbour, and Y. Kishiyama, "On regular resource grid for filtered ofdm," *IEEE Communications Letters*, vol. 20, no. 12, pp. 2486–2489, Dec 2016, doi:10.1109/LCOMM.2016.2572183.

[12] N. Michailow, M. Matthe, I. Gaspar, A. Caldevilla, L. Mendes, A. Festag, and G. Fettweis, "Generalized Frequency Division Multiplexing for 5th Generation Cellular Networks," *IEEE Transactions on Communications*, vol. 62, no. 9, pp. 3045–3061, Sept 2014, doi:10.1109/TCOMM.2014.2345566.

[13] D. Zhang, M. Matthe, L. Mendes, and G. Fettweis, "A study on the link level performance of advanced multicarrier waveforms under mimo wireless communication channels," *IEEE Transactions on Wireless Communications*, vol. PP, no. 99, pp. 1–1, 2017, doi: 10.1109/TWC.2017.2664820.

[14] N. Michailow, L. Mendes, M. Matthe, I. Gaspar, A. Festag, and G. Fettweis, "Robust WHT-GFDM for the Next Generation of Wireless Networks," *IEEE Communications Letters*, vol. 19, no. 1, pp. 106–109, Jan 2015, doi:10.1109/LCOMM.2014.2374181.

[15] L. Mendes, N. Michailow, M. Matthé, I. Gaspar, D. Zhang, and G. Fettweis, *Opportunities in 5G Networks A Research and Development Perspective*. CRC Press, 2016, Chapter 13 - GFDM: Providing Flexibility for the 5G Physical Layer, doi:10.1201/b19698-17.

[16] Z. Huang, Y. Ma, Y. Li, and G. Wen, "A low complexity sub-optimal approach to dynamic spectrum allocation for white space devices with heterogeneous bandwidth requirements," *IEEE Communications Letters*, vol. 21, no. 1, pp. 188–191, Jan 2017, doi: 10.1109/LCOMM.2016.2616863.

[17] G. Wunder, P. Jung, M. Kasparick, T. Wild, F. Schaich, Y. Chen, S. ten Brink, I. Gaspar, N. Michailow, A. Festag, L. L. Mendes, N. Cassiau, D. Ktenas, M. Dryjanski, S. Pietrzyk, B. Eged, P. Vago, and F. Wiedmann, "5GNOW: non-orthogonal, asynchronous waveforms for future mobile applications," *IEEE Communications Magazine*, vol. 52, no. 2, pp. 97–105, 2014, doi:10.1109/MCOM.2014.6736749.

[18] T. Rappaport, R. Heath, R. Daniels, and J. Murdock, *Millimeter Wave Wireless Communications*, ser. Prentice Hall Communications Engineering and Emerging Technologies Series from Ted Rappaport. Pearson Education, 2014. [Online]. Available: https://books.google.com.br/books?id=0Jh6BAAAQBAJ

[19] B. Panzner, W. Zirwas, S. Dierks, M. Lauridsen, P. Mogensen, K. Pajukoski, and D. Miao, "Deployment and implementation strategies for massive MIMO in 5G," in *2014 IEEE Globecom Workshops*, Austin, USA, Dec 2014, pp. 346–351, doi:10.1109/GLOCOMW.2014.7063455.

[20] M. S. Ali, "On the Evolution of Coordinated Multi-Point (CoMP) Transmission in LTE-Advanced," *International Journal of Future Generation Communication and Networking*, vol. 7, no. 4, pp. 91–102, Apr 2014, doi:10.14257/ijfgcn.2014.7.4.09.

[21] W. Ryan and S. Lin, *Channel Codes: Classical and Modern*. Cambridge University Press, 2009. [Online]. Available: https://books.google.com.br/books?id=0gwqxBU_t-QC

[22] S. Choi and K. G. Shin, "A class of adaptive hybrid ARQ schemes for wireless links," *IEEE Transactions on Vehicular Technology*, vol. 50, no. 3, pp. 777–790, May 2001, doi:10.1109/25.933312.

[23] N. Michailow and G. Fettweis, "Low peak-to-average power ratio for next generation cellular systems with generalized frequency division multiplexing," in *Proc. of IEEE Int. Symp. on Intelligent Signal Processing and Communications Systems (ISPACS)*, Nov. 2013, pp. 651–655, doi:10.1109/ISPACS.2013.6704629.

[24] M. Matthe, L. L. Mendes, I. Gaspar, N. Michailow, D. Zhang, and G. Fettweis, "Multi-user time-reversal STC-GFDMA for future wireless networks," *EURASIP Journal on Wireless Communications and Networking*, vol. 2015, no. 1, Dec. 2015, doi:10.1186/s13638-015-0366-6.

[25] D. A. Guimaraes, *Digital transmission: a simulation-aided introduction with VisSim/Comm*. Springer, 2009, doi:10.1007/978-3-642-01359-1.

[26] J. Peisa, S. Wagner, M. Sågfors, J. Torsner, B. Görsansson, T. Fulghum, C. Cozzo, and S. Grant, "High Speed Packet Access Evolution – Concept and Technologies," in *IEEE Vehicular Technology Conference (VTC Spring 2007)*, Sept 2007, pp. 819–824, doi:10.1109/VETECS.2007.178.

[27] T. Blajić, D. Nogulić, and M. Druẑijanić, "Latency Improvements in 3G Long Term Evolution," *Mipro CTI*, 2006. [Online]. Available: https://pdfs.semanticscholar.org/ed86/78a5572928049d23d4aa9bb7398b8d16b7b1.pdf

[28] T. Singal, *Wireless Communications*. McGraw-Hill Education Pvt Limited, 2010. [Online]. Available: https://books.google.co.in/books?id=cQJJzA8CCUUC

[29] 3GPP, "Summary of email discussion - Evaluation of extended DRX cycles for UEPCOP," *TSG-RAN WG2, R2-132893*, 2013. [Online]. Available: HTTP://www.3gpp.org/ftp/tsg_ran/WG2_RL2/TSGR2_83/docs/R\-2132393.zip

[30] T. Tirronen, A. Larmo, J. Sachs, B. Lindoff, and N. Wiberg, "Machine-to-machine communication with long-term evolution with reduced device energy consumption," *Transactions on Emerging Telecommunications Technologies*, vol. 24, no. 4, p. 413–426, Apr 2013, doi:10.1002/ett.2643.

[31] 3GPP, "Cellular system support for ultra-low complexity and low throughput Internet of Things (CIoT)(Release 13)," *3GPP TR 45.820 V13.1.0*, 2015. [Online]. Available: http://www.3gpp.org/ftp/Specs/archive/45_series/45.820/45820-d10.zip

[32] I. S. Gaspar, L. L. Mendes, N. Michailow, and G. Fettweis, "A synchronization technique for generalized frequency division multiplexing," *EURASIP Journal on Advances in Signal Processing*, vol. 2014, no. 1, p. 67, 2014, doi:10.1186/1687-6180-2014-67.

[33] H. Kim, J. Kim, S. Yang, M. Hong, M. Yoo, W. Lee, and Y. Shin, "An effective mimo-ofdm transmission scheme for ieee 802.22 wran systems." IEEE, 6 2008, doi:10.1109/CROWNCOM.2007.4549830.

[34] I. Gaspar, L. Mendes, M. Matthe, N. Michailow, A. Festag, and G. Fettweis, "LTE-compatible 5G PHY based on Generalized Frequency Division Multiplexing," in *11th International Symposium on Wireless Communications Systems (ISWCS)*, Aug 2014, pp. 209–213, doi:10.1109/ISWCS.2014.6933348.

[35] P. Harris, S. Zang, A. Nix, M. Beach, S. Armour, and A. Doufexi, "A distributed massive mimo testbed to assess real-world performance and feasibility," in *2015 IEEE 81st Vehicular Technology Conference (VTC Spring)*, May 2015, pp. 1–2, doi:10.1109/VTCSpring.2015.7145598.

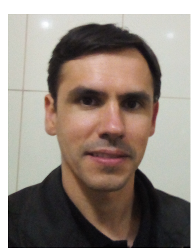

Juliano Silveira Ferreira received the B.Sc. and M.Sc. in electrical engineering from Inatel, Brazil, in 2002 and 2009, respectively. Since 2004 he works as a researcher and system specialist at Inatel, Brazil, were has been worked on several research projects funded by FAPEMIG and FINEP, besides projects in partnership with companies. His areas of interest include signal processing and communication systems engineering. Currently he is working on multicarrier modulations for 5G networks and future mobile communications systems.

Henry Douglas Rodrigues received the BSc. and MSc. in Electrical Engineer from Inatel, Brazil in 2003 and 2008, respectively. He is a doctorand in Electrical Engineer at Unifei, Brazil. In 2001 he joined Hitachi Kokusai Linear, as an R&D engineer on digital bradcasting systems, became project manager in 2011, and chief engineer in 2013. He contributed for the developement of high efficiency RF power amplifiers, modulators, multiplexers, and power amplifier linearization with digital pre-distortion. Since 2016 he is with Inatel, Brazil, as a reseracher on physical layer for 5G networks. His areas of interest include discrete-time signal processing, digital broadcasting, and communication systems engineering.

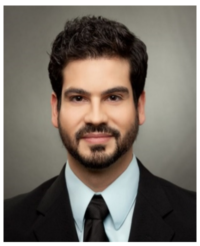

Arturo González received in 2008 his Bachelor of Science (B.Sc.) degree in Electronics and Communication Engineering from the Monterrey Institute of Technology (ITESM) in Mexico. During his Bachelor studies, he spend one semester abroad in Auckland University of Technology (AUT), focusing on radio communications. In 2011, he received his M.Sc. of Communication Engineering from the Technische Universität München. After his studies, he joined Nomor Research in Munich as a R&D engineer where he worked on QoS-Aware Radio Resource Management algorithms in LTE-Advanced relaying and LTE Protocol Stack development. In 2012, he joined the Fraunhofer Institute for Embedded Systems and Communication Technologies ESK in Munich where he performed research, simulation and prototyping of car-to-car communications over ad-hoc-plus-infrastructure networks. Since Janurary 2016 he is pursuing his PhD in the Vodafone Chair Mobile Communication Systems at Technische Universität Dresden. His current research focuses on Medium Channel Aspects and Radio Resource Allocation for 5G communications under heterogeneous QoS constraints.

Ahmad Nimr received his diploma in Communication Engineering from HIAST, Syria in 2004. Afterwards, he worked as a software and hardware developer from 2005 to 2011. Then, he perused a master of science in Communications and Signal Processing and obtained his M.Sc degree in 2014 from TU Ilmenau. His research at TU Ilmenau focused on tensor based signal processing. In addition, he contributed to the FP7 project EMPhAtiC. Since October 2015, he has been a member of Vodafone Chair Mobile Communication Systems, TU Dresden. He is currently carrying out research in low-latency multiple access and resources allocation techniques for 5G networks.

Maximilian Matthé received his Dipl.-Ing degree in Electrical Engineering from TU Dresden in 2013. During his studies he focused on mobile communication systems and communication theory. He performed his internship at National Instruments Dresden and worked on the design and implementation of a measurement site for LTE test UEs. In his Diploma Thesis he concentrated on waveform design for flexible multicarrier transmission systems. Since 2013 he is pursuing his PhD in the Vodafone Chair Mobile Communication Systems at Technical University Dresden. Maximilian's research focuses on the design and evaluation of MIMO architectures for future cellular networks.

Dan Zhang received the B.Sc. degree in electrical engineering from Zhejiang University, China in 2004, and both the M.Sc. and the Dr.-Ing. degree in Electrical Engineering and Information Technology from RWTH Aachen University, Aachen, Germany in 2007 and 2013, respectively. Her research interests are in the area of statistical signal processing, communication theory and optimization theory. During her PhD studies, she focused on iterative receiver designs. Since September 2014 she works as a post-doc researcher at Vodafone Chair Mobile Communications Systems at Technical University Dresden. She has worked on various national and international research projects with publication in journals, conference proceedings and workshops. Her current research focus is on the transceiver design of multicarrier waveforms with the objective of providing a new air interface for 5G networks.

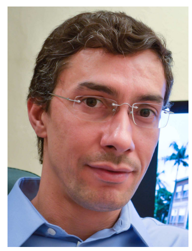

Luciano Leonel Mendes received the BSc. and MSc. in electrical engineering from Inatel, Brazil in 2001 and 2003, respectively. In 2007 he received the Doctor in electrical engineering degree from Unicamp, Brazil. Since 2001 he is a professor at Inatel, Brazil, where he has acted as technical manager of the hardware development laboratory from 2006 to 2012. He has coordinated the Master Program at Inatel and several research projects funded by FAPEMIG, FINEP and BNDES. He was a post-doc visiting researcher, sponsored by CNPq-Brasil, at Vodafone Chair Mobile Communications Systems at the Technical University Dresden from 2013 until 2015. His main area of research is wireless communication and currently he is working on multicarrier modulations for 5G networks and future mobile communications systems.

Gerhard P. Fettweis earned his Ph.D. under H. Meyr's supervision from RWTH Aachen in 1990. After one year at IBM Research in San Jose, CA, he moved to TCSI Inc., Berkeley, CA. Since 1994 he is Vodafone Chair Professor at TU Dresden, Germany, with 20 companies from Asia/Europe/US sponsoring his research on wireless transmission and chip design. He coordinates the 5G Lab Germany, and 2 German Science Foundation (DFG) centers at TU Dresden, namely cfaed and HAEC. Gerhard is IEEE Fellow, member of the German Academy of Sciences (Leopoldina), the German Academy of Engineering (acatech), and received multiple IEEE recognitions as well has the VDE ring of honor. In Dresden his team has spun-out sixteen start-ups, and setup funded projects in volume of close to EUR 1/2 billion. He co-chairs the IEEE 5G Initiative, and has helped organizing IEEE conferences, most notably as TPC Chair of ICC 2009 and of TTM 2012, and as General Chair of VTC Spring 2013 and DATE 2014.